Degradation and mechanism of 2,4-dichlorophenoxyacetic acid (2,4-D) by thermally activated persulfate oxidation

Jingju Cai [a], Minghua Zhou [a, *], Weilu Yang [a], Yuwei Pan [a], Xiaoye Lu [a], Karine Groenen Serrano [b]

[a] Key Laboratory of Pollution Process and Environmental Criteria, Ministry of Education, Tianjin Key Laboratory of Urban Ecology Environmental Remediation and Pollution Control, College of Environmental Science and Engineering, Nankai University, Tianjin, 300350, China
[b] Laboratoire de Génie Chimique, CNRS, INPT, UPS Université de Toulouse, 118 Route de Narbonne, F-31062, Toulouse, France

HIGHLIGHTS

- Thermally activated persulfate (TAP) could effectively degrade 2,4-D compared with Fe^{2+}/PS.
- TAP had higher TOC removal, longer radical duration time and wider pH applicability than Fe^{2+}/PS.
- A possible degradation pathway for 2,4-D was proposed.
- TAP was a promising method for removal of herbicide.

ARTICLE INFO

Keywords:
2,4-Dichlorophenoxyacetic acid
Thermally activated persulfate
Degradation mechanism
EPR
Fe^{2+}/PS

ABSTRACT

The chlorinated phenoxy herbicide of 2,4-dichlorophenoxyacetic acid (2,4-D) was oxidized by thermally activated persulfate (TAP). This herbicide was studied for different persulfate dosages (0.97–7.29 g L^{-1}), for varying initial pH levels (3–12) and temperatures (25–70 °C). Compared with Fe^{2+}/PS, TAP could achieve a higher total organic carbon (TOC) removal under wider pH ranges of 3–12. Increasing the mole ratio of PS to 2,4-D favored for the decay of 2,4-D and the best performance was achieved at the ratio of 50. The 2,4-D degradation rate constant highly depended on the initial pH and temperature, in accordance with the Arrhenius model, with an apparent activation energy of 135.24 kJ mol^{-1}. The study of scavenging radicals and the EPR confirmed the presence of both $SO_4^{\bullet-}$ and $^{\bullet}OH$. However, $SO_4^{\bullet-}$ was the predominant oxidation radical for 2,4-D decay. The presence of both Cl^- and CO_3^{2-} inhibited the degradation of 2,4-D, whereas the effect of NO_3^- could be negligible. Verified by GC/MS, HPLC and ion chromatography, a possible degradation mechanism was proposed.

1. Introduction

Nowadays, owing to the growing population and high demand for grain, there has been an increase in pesticide use in order to increase food production. These pesticides induce the contamination of both water and soil due to their refractory and toxic characteristics. In some agricultural wastewater the concentration of pesticides may be up to 500 mg L^{-1} (Huy et al., 2017; Jaafarzadeh et al., 2017a; Li et al., 2017a). In particular, 2,4-dichlorophenoxyacetic acid (2,4-D), one of the chlorinated phenoxy herbicides, has been widely used for controlling the weeds (Jaafarzadeh et al., 2017b; Jia et al., 2017). The presence of 2,4-D leads to the contamination of water that could result in causing cancer to humans and damaging to the environment. Therefore, the treatment of 2,4-D has received considerable interest for research, in order to reduce its menace to human health and the environment (Huy et al., 2017; Singh et al., 2017).

Recently, various advanced oxidation processes (AOPs) have been attempted to degrade 2,4-D, such as electrochemical (Zhu et al., 2012; Souza et al., 2016), electro-Fenton (Brillas et al., 2004; Casado et al., 2006), photocatalysis (Nie et al., 2015b; Mkhalid, 2016; Qiu et al., 2016), Fenton (Chen et al., 2015), ozonation (Rodríguez et al., 2017). Notably, in the late 1990s, *in situ* chemical oxidation (ISCO), which is based on strong oxidants such as ozone,

* Corresponding author.
E-mail address: zhoumh@nankai.edu.cn (M. Zhou).

https://doi.org/10.1016/j.chemosphere.2018.08.127

potassium permanganate and hydrogen peroxide, has received much attention due to its effective mineralization of recalcitrant organic compounds (Devi et al., 2016; Pan et al., 2016). In particular, persulfate ($S_2O_8^{2-}$), a promising alternative oxidant, has been extensively studied due to the following advantages: a high redox potential ($E^0 = 2.01$ V/SHE) (Deng et al., 2013; Li et al., 2017b; Matzek and Carter, 2016), activation to sulfate radical with a greater redox potential ($E^0 = 2.6$ V/SHE) and a longer lifetime (1000 fold) than $^{\bullet}OH$ radicals (Devi et al., 2016).

The approaches for persulfate activation include: heat energy (Nie et al., 2014; You et al., 2015; Peng et al., 2016b; Wang et al., 2016), alkaline pH (Liang and Guo, 2012), transition metals (Zhao et al., 2016; Ding et al., 2017), and ultrasound (Wang et al., 2015 ; Ye et al., 2016) through the Eqs. (1)–(3).

$$S_2O_8^{2-} + \text{heat/UV} \rightarrow 2\ SO_4^{\bullet-} \quad (1)$$

$$SO_4^{\bullet-} + OH^- \rightarrow SO_4^{2-} + {}^{\bullet}OH \quad (2)$$

$$S_2O_8^{2-} + Me^{n+} \rightarrow SO_4^{2-} + SO_4^{\bullet-} + Me^{(n+1)+} \quad (3)$$

Among these methods, transition metal like Fe^{2+} is the most common due to the relative nontoxicity, low cost and effectiveness. However, it is mostly used in acidic environments (pH 2—4) and is not effective for neutral and alkaline conditions. In addition, an excess of Fe^{2+} may jeopardize the degradation due to $SO_4^{\bullet-}$ quenching through Eq.(4) (Liang et al., 2013; Gu et al., 2017). Comparably, for TAP systems an increase in temperature could result in a faster generation of $SO_4^{\bullet-}$. Moreover, TAP is promising and highly effective for the degradation of hazardous contaminants (Liang et al., 2013; Ghauch et al., 2015; Yang et al., 2017). For the degradation of 2,4-D, though there are several researches on the abatement of 2,4-D using the method of TAP, for example, Kuśmierek and co-workers compared the various active method to decay 2,4-D, whereas only the effect of pH and PS concentration was studied (Kuśmierek et al., 2015). Liang and co-workers also observed the different activated ways to decay 2,4-D, while mainly focus on the Fe^{2+}/PS system (Liang et al., 2013). Therefore, there still have many unknown parameters that could further discuss.

$$Fe^{2+} + SO_4^{\bullet-} \rightarrow Fe^{3+} + SO_4^{2-} \quad (4)$$

Therefore, sulfate radicals, induced by TAP to treat 2,4-D was used. The objectives of this study were 1) to compare TAP with Fe^{2+}/PS to verify the feasibility and advantages of one or the other; 2) to investigate the important factors including PS dosage, temperature of the solution and initial pH; 3) to observe the predominant oxidation radicals in the TAP system under different conditions. 4) to explore the influence of some common anions involving Cl^-, CO_3^{2-} and NO_3^-; 5) to propose a possible degradation pathway for 2,4-D.

2. Experimental

2.1. Chemicals

2,4-D (Beijing, Lideshi chemical technology Co., Ltd, > 97%) was used as the target organic pollutant. Potassium persulfate (>99.5%) and NaCl (>99.8%) were purchased from Tianjin Guangfu technology development Co., Ltd. Sulfuric acid (H_2SO_4), sodium hydroxide (NaOH) (96%) and methanol (MeOH) (99.9%) were purchased from Tianjin Kemiou Chemical Reagent Co., Ltd. Phosphoric acid (85%) was obtained from Tianjin Wind Boat chemical reagents Technology Co., Ltd. Tert-butyl alcohol (TBA) (>99.5%) was purchased from the Sinopharm Group Chemical Reagent Co., Ltd. (Shanghai, China). $NaNO_3$, Na_2CO_3 (>99.8%) and $FeSO_4$ (>99%) were purchased from Tianjin Yongda chemical reagents development center. 5,5-Dimethyl -1- pyridine N-oxide (DMPO) (Shanghai Aladdi biological technology Co., Ltd) was used to scavenge $SO_4^{\bullet-}$ and $^{\bullet}OH$ to test electron paramagnetic resonance (EPR).

2.2. 2, 4-D degradation

The degradation experiments were carried out in a beaker with thermostatic equipment (DF-101S) to control the working temperature of 20—70 °C. 100 mL of 2,4-D (100 mg L^{-1}) was added into the reactor then it was placed into the thermostatic equipment and stirred. PS powder ranging from 0.096 g—0.72 g (3.6 mM- 27 mM) was added into the reactor when the temperature reached the desired one. In some experiments, initial pH (3—12) was adjusted with NaOH (0.1 mol L^{-1}) and H_2SO_4 (0.1 mol L^{-1}). In order to investigate the effects of inorganic ions, the solution was pre-added with the Cl^-, CO_3^{2-} and NO_3^-. Methanol and TBA were employed as radical scavengers, and the mole ratios between MeOH and PS, and between TBA and ps were 400:1. DMPO was selected as the trapping agent due to the fact that it could react with radical intermediates ($SO_4^{\bullet-}$ and $^{\bullet}OH$) to form stable radical adducts that can be detected by EPR technology. For this, 80 μL DMPO (100 mM) was firstly stored in a centrifuge tube, then 40 μL samples were added to the existing tubes, and tested immediately. In the Fe^{2+}/PS system, persulfate powder was firstly fully mixed with 2,4-D solution, then Fe^{2+} was added to the solution. Regularly, approximately 1.5 mL solution was sampled and filtered through a 0.22 μm membrane filter to be analyzed.

2.3. Analysis methods

The concentration of 2,4-D was determined by High Performance Liquid Chromatography (FL2200-2) with a Beckman ODS C18 column (5 μm, φ4.6 × 250 mm) at a flow rate of 1.0 mL min^{-1} coupled with a UV detector at a wavelength of 280 nm. The mobile phase consisted of 60:40 v/v methanol/0.2% phosphoric acid. A gas chromatography (Agilent 7890A, California, USA)/mass spectrometry (Agilent 5975C) (GC/MS) system was equipped with a HP-5MS column (30 m, φ0.25 mm × 0.25 μm) and the carrier gas was helium with a flow rate of 1.0 mL min^{-1}. The original temperature was 35 °C, which was held for 1 min. Then the temperature was increased to 300 °C at a rate of 10 °C/min and held for 1 min. The injection volume was 1 μL. Both the injector and detector temperatures were 280 °C. Chloride (Cl^-) and small molecule acids were measured through an ion chromatograph (IC) (Dionex ICS-900, USA) coupling an IonPac AS11-HC (φ4 × 250 mm) column and DS5 conductivity detector. Total organic carbon (TOC) was measured with an TOC-V_{CSN} instrument (Shimadzu). EPR measurements of radicals were carried out on a MiniScope MS400 (Freiberg Instruments, Germany), the center field was 320 mT with a range of 10 mT. The degradation efficiency (η/%) of 2,4-D was calculated according to Eq. (5),

$$\eta = \frac{C_0 - C_t}{C_0} \times 100\% \quad (5)$$

Where, C_0 and C_t are the initial concentrations of 2,4-D (mg L^{-1}) and concentration at reaction time *t*.

3. Results and discussion

3.1. Degradation of 2,4-D by Fe^{2+}/PS system

In the Fe^{2+}/PS system, the effect of mole ratio between Fe^{2+} and

PS (18 mM) ($[Fe^{2+}]_0/[PS]_0 = 1{:}18$ to 6:18) was investigated and the decay of 2,4-D was very fast in the first minute then much slower in 1 h (Fig. S1). The increase Fe^{2+} concentration from 1 mM to 2 mM led to an increasing removal from 60.7 to 76.8% during the first minute. After that, the removal of 2,4-D was delayed due to the consumption of Fe^{2+}, stopping the PS activation (Nie et al., 2015a). When the concentration of Fe^{2+} was increased to 3 mM, the removal efficiency of 2,4-D was 90.5% in 1 min. However, when the concentration of Fe^{2+} was 4–6 mM, the increase in 2,4-D removal was much slower. This may be due to the excessive Fe^{2+} working as a scavenger of $SO_4^{\bullet-}$ (Oh et al., 2009). Therefore, 3 mM of Fe^{2+} was selected for further comparison with TAP.

3.2. Comparison between Fe^{2+}/PS and TAP

As shown in Fig. 1a, only 2% of 2,4-D was degraded with PS alone at 25 °C in 1.5 h. When heated at 60 °C without PS, only 1% of 2,4-D was degraded. When heated at 60 °C with PS, 97% of 2,4-D was removed within 1.5 h. For Fe^{2+}/PS, even though 2,4-D was quickly degraded, less TOC was removed (8.7%) than TAP (45%) in 60 min.

To explore the possible reasons for this, EPR was conducted in Fe^{2+}/PS and TAP systems. The DMPO-OH adducts showed the characteristic 1: 2: 2: 1 quartet (Fang et al., 2017), and DMPO-SO_4 adducts displayed the six peaks as 1: 1: 1: 1: 1:1 (Chen et al., 2017b), indicating the simultaneous existence of $SO_4^{\bullet-}$ and $^{\bullet}OH$. These results correlated with other reports (Duan et al., 2016; Kang et al., 2016). As shown in Fig. 1b, in Fe^{2+}/PS, process radicals were quickly produced whereas they also quickly disappeared. At 30 s, the intensity of $SO_4^{\bullet-}$ and $^{\bullet}OH$ was strong, whereas at 1 min the intensity decreased quickly. At 2 min the signal was very weak, and after 2 min the intensity of radicals approached the blank (the data was not provided). This is why 84% of 2,4-D could be removed by Fe^{2+}/PS within 30 s, howbeit it increased to 90% in 2 min. However, in the TAP system, though at the beginning the signal of $SO_4^{\bullet-}$ and $^{\bullet}OH$ was weak, at 1 min the signal increased quickly, and at 3 and 8 min the signal did not show a tendency to decrease (Fig. 1c). At 8 min the removal of 2,4-D for Fe^{2+}/PS was better than for TAP, whereas the oxidation potential for TAP was higher than that for Fe^{2+}/PS. Overall, Fe^{2+} activated PS was a rapid and short process, whereas in TAP, it was a continuous strengthening process due to the heat energy. Therefore, better TOC removal was observed for the TAP process than for the Fe^{2+}/PS, confirming the effectiveness of the former.

Table 1 lists the comparison of different AOPs methods to remove 2,4-D. For the electrochemical advanced oxidation processes (EAOPs), for example, the electrochemical oxidation or the combined methods such as electro-Fenton/BDD, though the rate constant of degradation was high, the TOC removal efficiency was low (Zhao et al., 2010). For the eletrochemical activation of PS, as listed in Fig. S2, the increase in the current density accelerated the degradation of 2,4-D meanwhile the side reactions were also enhanced, and thus led to an increase in energy consumption (Bu et al., 2018). So 10 mA/cm^2 was selected for the comparison. At this condition the rate constant and TOC removal rate were both lower than the method of TAP. According to the degradation rate constant in this work (0.186 min^{-1}), the oxidation rate was higher than those by the combined methods including the hydrothermal electrocatalytic oxidation method (0.0303 min^{-1}) which needed a much higher temperature, the photo-degradation method ($ZnIn_2S_4$/g-C_3N_4), FeS/H_2O_2, TiO_2/UV, TiO_2/O_3/UV and nano-Fe_2O_3 catalysis (Giri et al., 2010; Chen et al., 2015; Qiu et al., 2016; Jaafarzadeh et al., 2017a; Kermani et al., 2018). Therefore the TAP system was an efficient method to treat 2,4-D.

3.3. Effect of persulfate dosage

In the TAP system, the amount of PS plays an important role. Therefore different mole ratios between PS and 2,4-D (8, 12, 20, 30, 40, 50, 60) were studied. As shown in Fig. 2, when the ratio was 8 and 12, only 58.2% and 74% 2,4-D was oxidized for the reaction time of 180 min, respectively. However, further increased the ratio from 20 to 60, the complete removal of 2,4-D achieved for the reaction time of 210 min, 120 min, 90 min and 60min, respectively. The best performance was recorded for ratio 50. The degradation of 2,4-D correlated well to a pseudo-first-order kinetics model, as described in Eq. (6)

$$-\frac{d[2,4-D]}{dt} = k[2,4-D] \tag{6}$$

Where k is the pseudo-first-order rate constant (s^{-1}), and [2,4-D] is the concentration of 2,4-D (mg L^{-1}). The rate constant increased as the ratio improved from 8 to 50 (8.3×10^{-5} to 1.4×10^{-3} s^{-1}) then decreased at ratio of 60 (1.0×10^{-3} s^{-1}). From ratio 8 to 50, $t_{1/2}$ was shortened from 2.32 h to 8.25 min (Table S1). Based on these results that the rate of 2,4-D could be enhanced by an increase of persulfate concentration to some extent. Normally, at a high ratio, more $SO_4^{\bullet-}$ would be generated whereas the excess $SO_4^{\bullet-}$ may scavenge $SO_4^{\bullet-}$ due to the high reaction rate described in Eq. (7) (Peng et al., 2016a). It can explain the decrease in performance for the ratio of 60.

$$SO_4^{\bullet-} + SO_4^{\bullet-} \rightarrow S_2O_8^{2-} \qquad k = 4.0 \times 10^8\ M^{-1}\ s^{-1} \tag{7}$$

3.4. Effect of temperature

Fig. 3a shows the degradation efficiency of 2,4-D under different temperatures from 50 to 70 °C at pH 3.5 as a function of reaction time. As seen the 2,4-D oxidized was 86.3% during the reaction time of 180 min. However, when the temperature increased from 50 to 70 °C a significant difference on performance was observed. For example, the complete removal of 2,4-D was obtained at 90 min, 50 min, 30 min periods for the temperature of 60, 65 and 70 °C, respectively. This result indicated that the degradation efficiency of 2,4-D depended on the temperature. Besides, the degradation of 2,4-D at 50, 60, 65 and 70 °C was fitted with a pseudo-first-order kinetics model, obtaining the rate constant of 0.612, 3.168, 5.76, and 11.16 h^{-1}, respectively. The half-life decreased from 1.13 h to 3.6 min (Table S2) which was due to the fact that increasing the temperature resulted in a more active species of radicals (Gao et al., 2016). Meanwhile, Fig. 3b indicates that when temperature was increased from 50 to 70 °C, the intensity of the adducts of $SO_4^{\bullet-}$ and $^{\bullet}OH$ improved, which also verified the previous study. As seen from the insert panel of Fig. 3a, the degradation of 2,4-D correlated well with the Arrhenius behavior, resulting in a good linear relation with a function that can be written as Eq. (8):

$$\ln(k) = \ln A - E_a/RT \tag{8}$$

where A is the Arrhenius constant, E_a is the apparent activation energy (kJ mol^{-1}), R is the universal gas constant (8.314×10^{-3} kJ mol^{-1} K^{-1}), and T is the absolute temperature (K). This correlation enables the determination of the apparent activation energy which is 135.24 kJ mol^{-1} close to the ones obtained for the degradation of *p*-nitrophenol, Naproxen, Carbamazepine, Triclosan, 1,1,1-Trichloroethane and Phenol by TAP as listed in Table 2 (Gu et al., 2011; Ghauch et al., 2015; Chen et al., 2016; Gao et al., 2016; Kang et al., 2016; Ma et al., 2017), while lower than

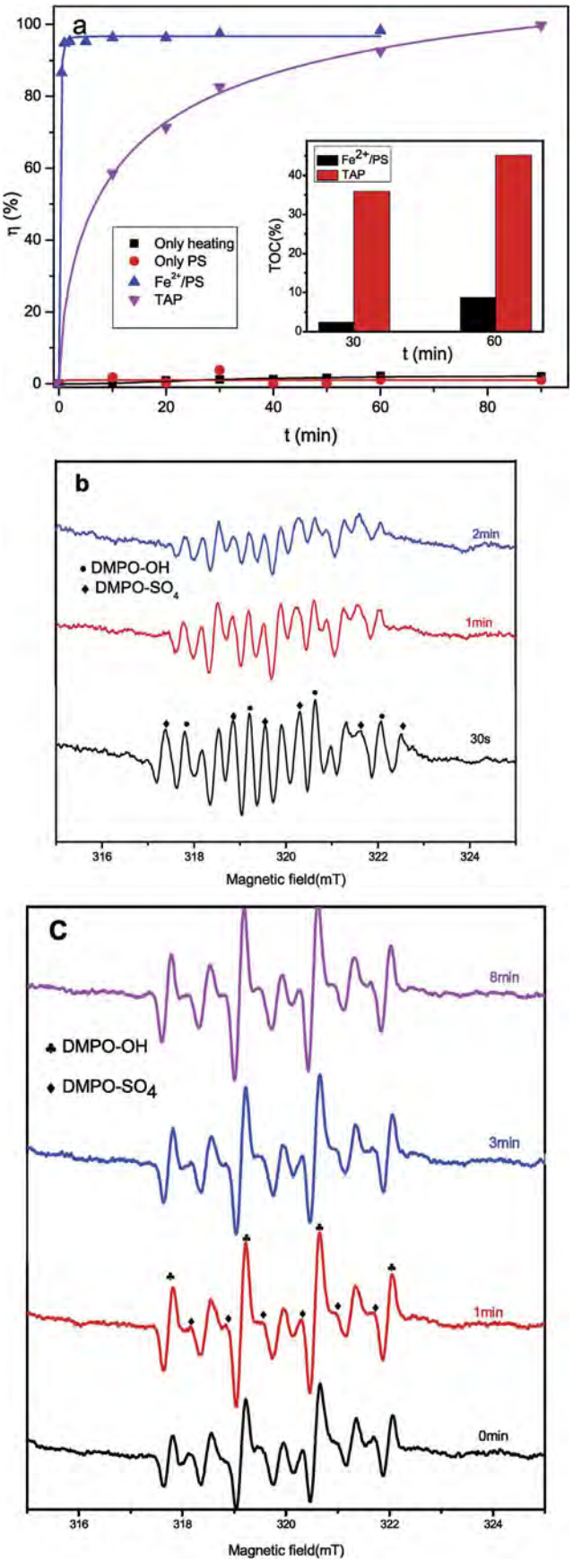

Fig. 1. (a) Comparison between TAP/PS and Fe^{2+}/PS. Conditions: For TAP, 2,4-D (0.45 mM), PS 18 mM, T = 60 °C pH 3.5. For Fe^{2+}/PS, Fe^{2+} 3 mM, PS 18 mM, pH 3.5 (b) Influence of time on the radicals in Fe^{2+}/PS, PS 10 mM, DMPO 100 mM, pH 3.5, T = 20 °C (c) Influence of time on the radicals in TAP, PS 10 mM, DMPO 100 mM, pH 3.5, T = 60 °C.

Bisphenol A (Olmez-Hanci et al., 2013), higher than Decabromodiphenyl ether and Fluconazole (Peng et al., 2016a; Yang et al., 2017). Ma and co-workers revealed that under the same phenol concentration, PS concentration and active temperature, the E_a decreased with the increase in the solution pH, however, under the same pH, increasing the PS concentration did not affect the value of E_a. This indicated that different reaction conditions had a significant influence on E_a (Ma et al., 2017). In addition, as observed from Table 2, different compounds and reaction systems also influenced the E_a.

3.5. Effects of initial pH

For TAP, the initial pH of the solution has an important effect on the existing form of radicals (Liang et al., 2013). Therefore, tests to study the effect of the initial solution pH (3–12) on 2,4-D degradation were conducted under the temperature of 60 °C and PS concentration of 18 mM, and the results are depicted in Fig. 4. The applied pH dropped to the close value between 2.11 and 2.45 after reaction, meaning that all the reaction conditions were under the same one due to the release of H^+ coming from the reaction between $SO_4^{\cdot-}$ and H_2O or OH^- (Chen et al., 2017a). Fig. 4 shows that the degradation efficiency of 2,4-D was highly depended on the initial pH. Both a pH of 3 and an unadjusted pH could accelerate 2,4-D decay with a maximum rate constant of 0.075 and 0.077 min^{-1}, respectively. Whereas, when the pH was between 5 and 12, it had an inhibiting effect based on the rate constant that decreased from 0.051 to 0.031 min^{-1}. This results was in accordance with the oxidation of carbamazepine and chloramphenicol, in which the increase in the pH resulted in the decreased rate constant (Nie et al., 2014; Yang et al., 2017).

The following mechanisms may contribute to the effect of pH: 1) It was reported by Deng et al. that more sulfate radicals could be generated through acid-catalysis, whereas for higher pHs the role of acid-catalysis would be weakened (Deng et al., 2013) and the sulfate radicals may be consumed by the hydroxyl ions when increasing the pH (Nie et al., 2014). 2) Under alkaline conditions, because of the high redox potential of ·OH which became the dominant radical species, the degradation of 2,4-D was inhibited due to the SO_4^{2-} scavenging ·OH (Gao et al., 2016). Besides, due to the short lifetime of ·OH, it can not effectively react with 2,4-D (George et al., 2001). 3) Under alkaline conditions, during the mineralization of 2,4-D, there may generate some bicarbonate and carbonate that can inhibit the reaction, and this mechanism was confirmed in section 3.7. Therefore, the acidic condition was favor for the degradation of 2,4-D.

3.6. Identification of predominant oxidation radical species in the TAP system

For TAP oxidation system, once PS was activated it not only produce $SO_4^{\cdot-}$ but also the ·OH through the reaction with H_2O (Anipsitaks et al., 2006 . According to the previous studies, oxidation of contaminant via $SO_4^{\cdot-}$ is more favorable to electron transfer. Whereas for the case of ·OH, the hydrogen addition or abstraction may take place (Anipsitaks and Dionysiou, 2004). Therefore, in order to identify the radical species responsible for the oxidation of 2,4-D, a quenching study was conducted at pH 3 and 12 using excess MeOH and TBA as the scavenging agents. MeOH had a comparable rate between ·OH ($1.2–2.8 \times 10^9\ M^{-1}\ s^{-1}$) and $SO_4^{\cdot-}$

Table 1
Performance comparison with literatures.

Methods	Experimental conditions	C_0 (mg/L)	t (min)	η (%)	TOC (%)	k (min^{-1})	references
Photodegradation	0.4 g/L 20% $ZnIn_2S_4$/g-C_3N_4	100	180	90	41.6	0.0129	(Qiu et al., 2016)
TiO_2/O_3/UV	TiO_2 loading, 5.0 g L^{-1}, O_3 42 ppm UV lamp 10 W	10	80	100	43	0.092	(Oyama et al., 2009)
TiO_2/UV	TiO_2 fiber, UV lamp 10 W	100	120	55	25	0.0046	(Giri et al., 2010)
FeS/H_2O_2	10 mM H_2O_2, FeS 0.5 g/L, pH 4.5, 50 °C	10	300	94.9	70.4	0.0241	(Chen et al., 2015)
hydrothermal electrocatalytic oxidation	Current density 5 mA/cm^2, 135 °C, Pt cathode, Pt anode	100	180	93.7	99.8	0.0303	(Xiao et al., 2016)
Electrochemical oxidation	BDD cathode, titanium anode, Current density 9.7 mA/cm^2	100	120	86.5	60	1.14	(Zhao et al., 2010)
EF/BDD	pH 3, cathode and anode BDD,Fe^{2+} 0.7 mM, current density 15 mA/cm^2, flow rate 10 L/min	60	160	70	83	0.309	(García et al., 2013)
heterogeneous catalysis	PMS 3.0 mM, nano-Fe_2O_3 0.5 g/L, pH 6.0	20	60	52.3	26.5	0.0267	(Jaafarzadeh et al., 2017a)
heterogeneous catalysis	PS 20 mM, pH 3.0, nano-Fe_2O_3 0.5 g/L, T 50 °C	200	120	78	68	0.0059	(Kermani et al., 2018)
Electrochemical Activation of PS	pH 3.5, current density 10 mA/cm^2, PS 18 mM	100	120	100	25.2	0.052	This work
TAP	T 70 °C, pH 3.5, PS 18 mM	100	300	100	94.5	0.186	This work

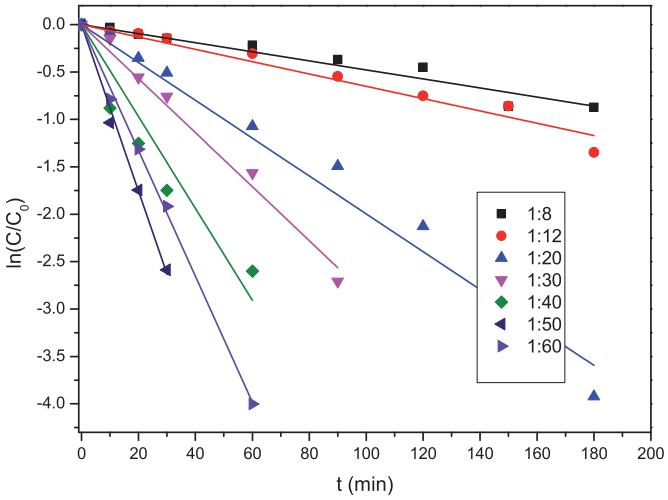

Fig. 2. Influence of the ratio between 2,4-D and persulfate concentration. Conditions: 2,4-D (0.45 mM), pH 3.5, T 60 °C.

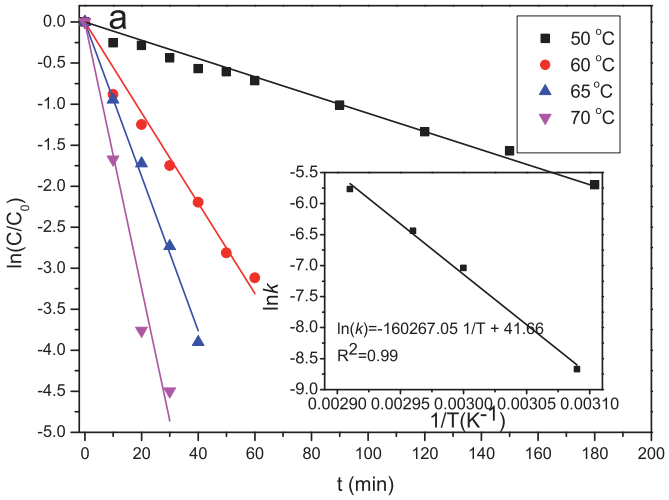

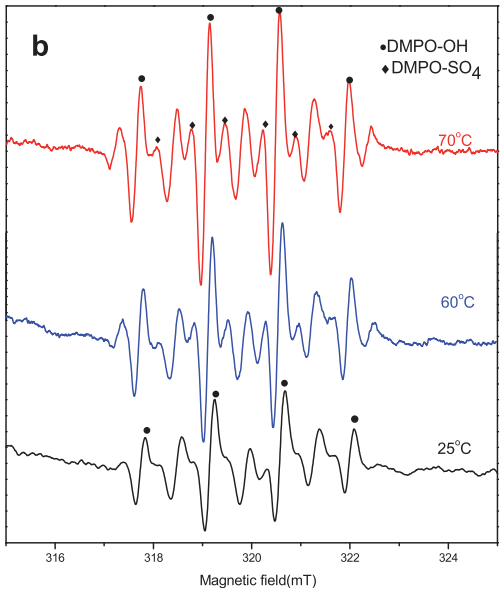

Fig. 3. Influence of temperature (a) on the removal of 2,4-D (0.45 mM), PS 18 mM, pH 3.5. (b) On intensity of radicals, PS 10 mM, DMPO 100 mM, pH 3.5.

($1.6–7.7 \times 10^7\ M^{-1}\ s^{-1}$). Meanwhile TBA had a rate of $3.8–7.6 \times 10^8\ M^{-1}\ s^{-1}$ with $^{\bullet}OH$ whereas only $4.0–9.1 \times 10^5\ M^{-1}\ s^{-1}$ with $SO_4^{\bullet-}$ (Rao et al., 2013; Liu et al., 2017). Hence MeOH was the scavenger for $SO_4^{\bullet-}$ and $^{\bullet}OH$, and TBA was supposed to scavenge only $^{\bullet}OH$.

As depicted in Fig. 5a and b, when MeOH or TBA was added at initial pH 3 and 12, the rate constant was significantly decreased, and decreased more in the case of TBA was added. As shown in Table 3, the changes of rate constant (R%) was calculated through Eq. (9) : in the presence of TBA, the R% value was −36.5% and −43.2. %, but for the case of MeOH, the R% value was −84.6% and −92.9% at pH 3 and 12, respectively. In the presence of MeOH, both $SO_4^{\bullet-}$ and $^{\bullet}OH$ were scavenged howbeit the excess TBA only consume $^{\bullet}OH$. This results illustrated that $SO_4^{\bullet-}$ was probably the predominant radical at pH 3 and 12. This phenomenon denoted that whether in acidic or alkaline initial pH conditions $SO_4^{\bullet-}$ was the predominant radical for 2,4-D degradation due to the fact that in alkaline conditions $SO_4^{\bullet-}$ could be converted into $^{\bullet}OH$ (Eq. (10)), which was inversely inhibited by the background SO_4^{2-}. Therefore, $SO_4^{\bullet-}$ plays a more important role in the TAP system for 2,4-D decay. This was consistent with the works of Ghauch et al. (2015).

$$R\% = \left(k_{with\ scavenger} \Big/ k_{without\ scavenger} - 1\right) \times 100 \quad (9)$$

$$SO_4^{\bullet-} + OH^- \rightarrow SO_4^{2-} + {}^{\bullet}OH \quad \text{alkaline condition} \quad (10)$$

Table 2
Activation energy comparison with published literatures.

Compound	Initial concentration	T (°C)	PS (mM)	pH	System	*Ea* (kJ mol^{-1})	Reference
Naproxen	50 μM	40–70	1 mM	7.8	aqueous	155 ± 26.4	(Ghauch et al., 2015)
Bisphenol A	88 μM	40–70	10 mM	6.5	aqueous	184 ± 12	(Olmez-Hanci et al., 2013)
Carbamazepine	40 μM	40–70	1 mM	5.13	aqueous	120.4 ± 2.6	(Deng et al., 2013)
p-Nitrophenol	93 (±2) mg kg^{-1}	40–80	60 mM kg^{-1}	–	soil	133.7	(Chen et al., 2016)
Triclosan	31 μM	50–80	0.155 mM	8	Under ground	121.12	(Gao et al., 2016)
1,1,1-Trichloroethane	0.15 mM	20–50	15 mM	4.8	Ground water	122.44	(Gu et al., 2011)
Phenol	1 mM	30–70	20 mM	3.6	aqueous	139.3 ± 11.1	(Ma et al., 2017)
Decabromodiphenyl ether	20 mg kg^{-1}	50–70	500 mM	3	soil	16.4	(Peng et al., 2016a)
Fluconazole	10 mg L^{-1}	30–60	10 mM	5	aqueous	37.8	(Yang et al., 2017)
2,4-D	0.45 mM	50–70	18 mM	3.5	aqueous	135.24	This work

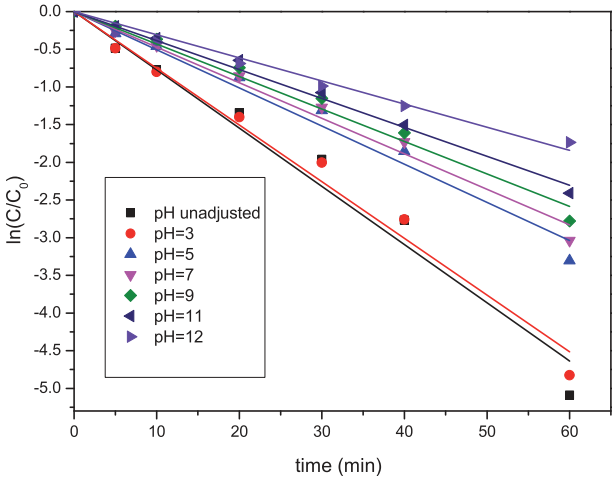

Fig. 4. Influence of pH (a) on the removal of 2,4-D (0.45 mM), PS 18 mM, T 60 °C.

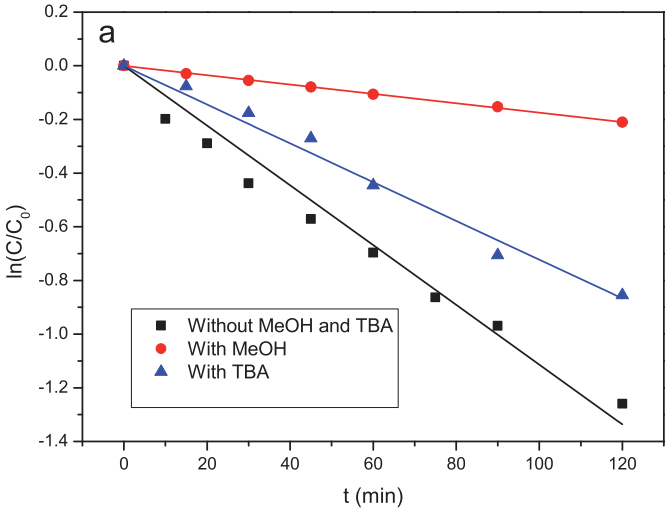

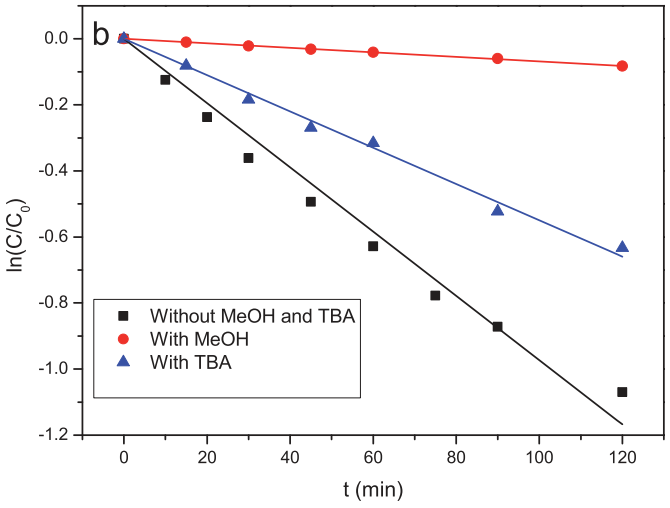

Fig. 5. (a) Trapping study at pH 3, 2,4-D (0.45 mM), PS 5 mM, T 60 °C, MeOH:PS = 400:1, TBA: PS = 400:1. (b) Trapping study at pH 12, 2,4-D (0.45 mM), PS 5 mM, T 60 °C, MeOH:PS = 400:1, TBA: PS = 400:1.

3.7. *Effect of anions*

Many organic pollutants co-exist with some anions, hence it is important to investigate the influence of ions in the TAP process. Moreover, the opinions on the effect of ions are still being debated. Gao et al. observed that a low level of chloride ions could accelerate the degradation of Triclosan, while over 10 mM caused an inhibiting effect (Gao et al., 2016). Fang et al. found that the presence of chloride greatly inhibited the transformation of 2,4,4-trichlorobiphenyl and biphenyl (Fang et al., 2012). Therefore it is imperative to explore the role of chloride ions on the degradation of 2,4-D. As shown in Fig. 6a, the presence of chloride inhibited the degradation of 2,4-D, in which the removal efficiency in 1 h decreased from 84% to 40% when the concentration of chloride increased from 0 to 50 mM (the significant Cl^- source from dechlorination of 2,4-D could not be ignored). The degradation rate constant also supported this decrease from 0.0286 min^{-1} to 0.00915 min^{-1} (insert Fig. 6a). This might be explained by the fact that Cl^- could react with $SO_4^{\bullet-}$ to form $Cl^{\bullet}$, $Cl_2^{\bullet-}$ and $ClHO^{\bullet}$, whereas these radicals had a much weaker oxidation potential than $SO_4^{\bullet-}$ (Fang et al., 2012). Therefore, the inhibit effect was observed.

In addition, the carbonate ion is also an important ion in the environment which could act as a scavenger for the $SO_4^{\bullet-}$, as described in Eqs. (7) and (8) (Zhao et al., 2016). Carbonate ions could also be found in the form of bicarbonates. The forms depend on the pH of the solution through Eqs.(11-12).

$$H_2CO_3 \rightarrow H^+ + CO_3^{2-} \qquad pKa = 6.37 \qquad (11)$$

Table 3
The changes of R% value under different pH.

Scavenger	pH = 3 (R%)	pH = 12 (R%)
MeOH	−84.6	−92.9
TBA	−36.5	−43.4

$$HCO_3^- \rightarrow H^+ + CO_3^{2-} \qquad pKa = 10.33 \qquad (12)$$

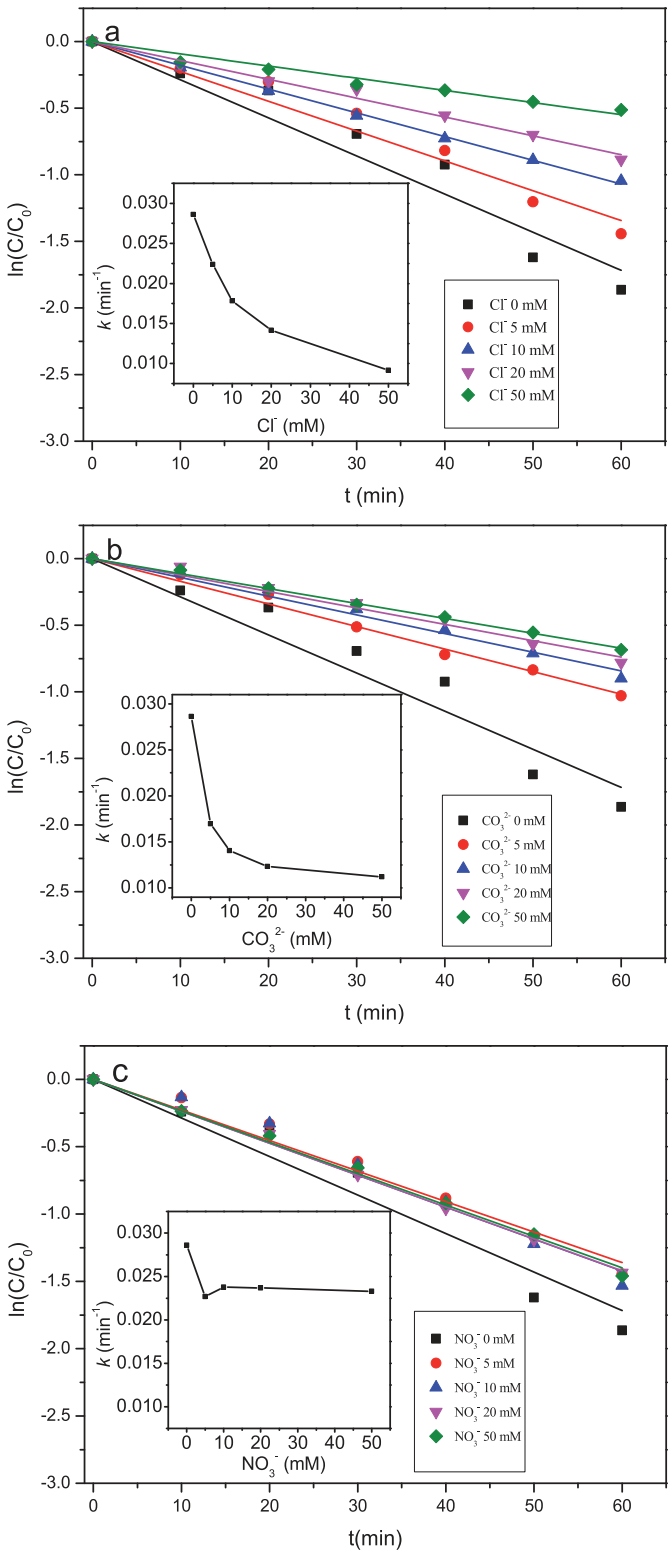

Fig. 6. (a) Influence of Cl^-, 2,4-D (0.45 mM), PS 18 mM, pH 3.5, T 60 °C. (b) Influence of CO_3^{2-}, 2,4-D (0.45 mM), PS 18 mM, pH 3.5, T 60 °C. (c) Influence of NO_3^-, 2,4-D (0.45 mM), PS 18 mM, pH 3.5, T 60 °C.

As shown in Fig. 6b, when carbonate ions concentration were added from 5 to 50 mM, the rate constant was decreased from 0.0286 min^{-1} to 0.0112 min^{-1}. This indicated that carbonate ions had an inhibit effect on the decay of 2,4-D. Due to the scavenge reaction, carbonate ions will decrease the sum of $SO_4^{\bullet-}$, and therefore, the degradation efficiency reduced from 84% to 50% in 1 h.

$$SO_4^{\bullet-} + CO_3^{2-} \rightarrow CO_3^{\bullet 2-} + SO_4^{2-} \qquad k = 1.6 \times 10^6\ M^{-1}\ s^{-1} \tag{13}$$

$$SO_4^{\bullet-} + HCO_3^- \rightarrow HCO_3^{\bullet-} + SO_4^{2-} \qquad k = 6.1 \times 10^6\ M^{-1}\ s^{-1} \tag{14}$$

The effect of nitrate ions, with a concentration of 5–50 mM was investigated. As seen in Fig. 6c, nitrate ions had almost no influence on the degradation rate constant (from the inset Fig. 6c). This is reasonable since nitrate ions only slightly react with $SO_4^{\bullet-}$ ($5.0 \times 10^4\ M^{-1}\ s^{-1}$) (Nie et al., 2014) and cannot induce a pH change of the solution. Therefore, the effect of the nitrate ion on the degradation of 2,4-D is negligible.

4. Possible degradation pathway of 2,4-D in the TAP system

The intermediates were identified by HPLC, GC/MS, and IC during the degradation of 2,4-D. The GC/MS results revealed that the intermediates were 2,4-DCP, 2,6-DCP, 2,4,6-trichlorophenol, 2-chlorohydroquinone, 2-chloro-1,4-benzoquinone (as shown in Fig. 7a). Furthermore, HPLC and IC detected some small acid molecules, such as glycolic acid, fumaric acid and oxalic acid. In addition to 2,4,6-trichlorophenol, the other intermediates were consistent with other reports (Kwan and Chu, 2004; Xu and Wang, 2012; Lam et al., 2015; Chen et al., 2017a). The formation of 2,4,6-trichlorophenol could be due to the generation of $Cl^{\bullet}$ from Cl^-, which was released during degradation and reacted with $SO_4^{\bullet-}$ and $^{\bullet}OH$.

Based on the above results, a possible degradation pathway was proposed in Fig. 7c. 2,4-DCP was the first intermediate which correlated with the result of García et al. (2013). In addition, the presence of the by-product benzoquinone was also confirmed by the authors. From the Fig. 7b, the dechlorination rate and the removal rate of TOC increased continuously, indicating that the degradation of 2,4-D was both a dechlorination and a mineralization process. Owing to the role of $SO_4^{\bullet-}$ and $^{\bullet}OH$, 2,4-DCP formed 2-chlorohydroquinone, and then generated 2-chloro-1,4-benzoquinone. This then resulted in the formation of benzoquinone through dechlorination. Another possible pathway could be due to the role of $Cl^{\bullet}$, the ortho position of 2,4-DCP would be substituted to produce 2,4,6-trichlorophenol. Then through the hydroxylation and dechlorination, 2,6-DCP was gradually produced and further converted into benzoquinone, which could open the ring to form oxalic acid and formic acid, until finally being mineralized to CO_2 and H_2O.

5. Conclusions

Compared with conventional Fe^{2+}/PS, the degradation of 2,4-D by TAP achieved a better performance. In the TAP system, both acidic conditions and high temperatures favor the degradation of 2,4-D. For the initial PS concentration, the best one was 22.5 mM, whether in acidic or alkaline conditions, sulfate radicals were the predominant oxidation species. Anions in the solution, such as Cl^- and CO_3^{2-}, inhibited the degradation of 2,4-D. Based on the detected intermediates, a possible degradation mechanism by TAP was proposed. The TAP system is a promising method to treat 2,4-D. It has the possibility for practical application especially for hot wastewater, which could reduce the treatment cost.

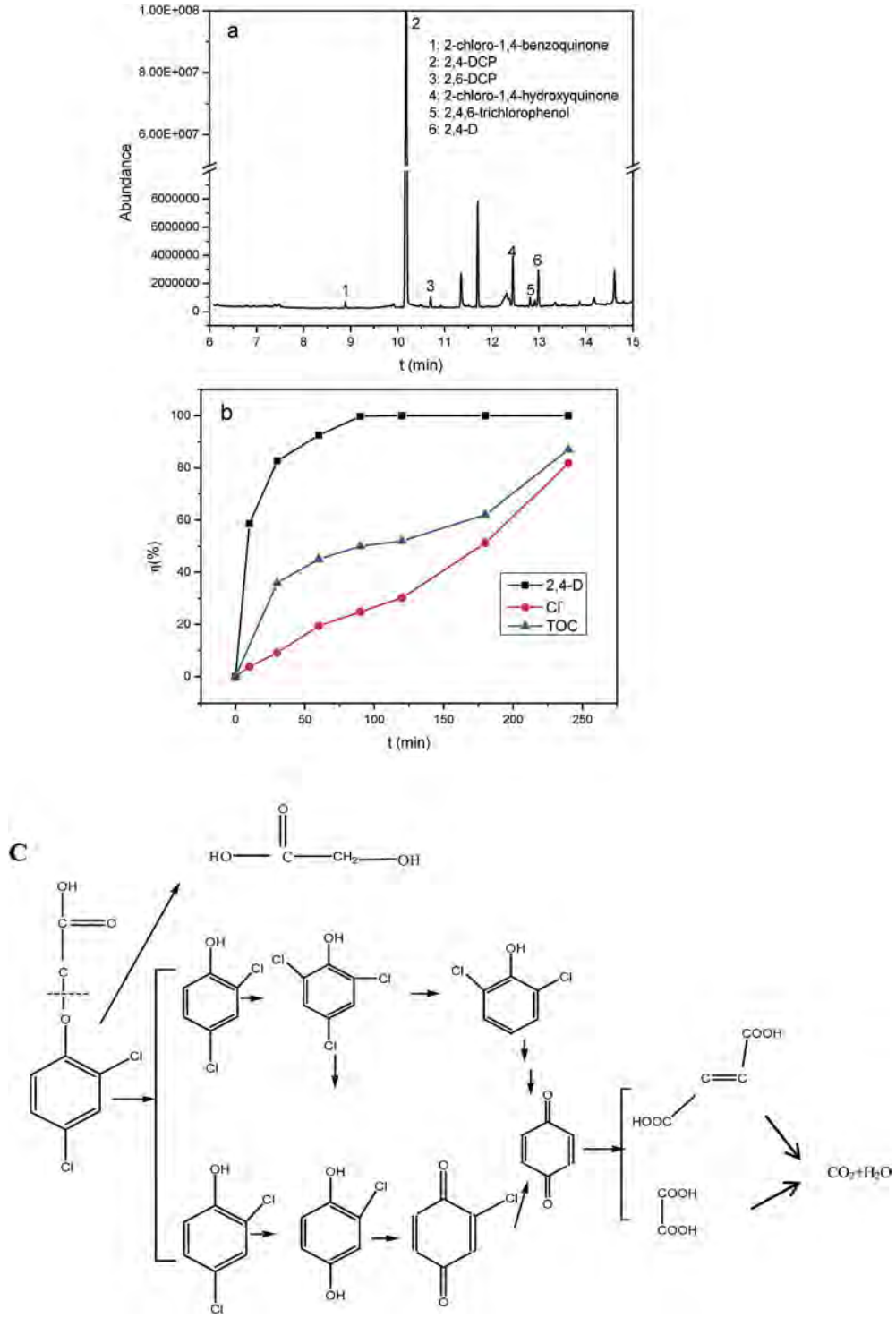

Fig. 7. (a) GC/MS result of the intermediates of 2,4-D degradation, (b) the changes of 2,4-D, Cl^- and TOC, (c) the possible pathway of 2,4-D. Conditions: 2,4-D (0.45 mM), PS 18 mM, pH 3.5, T 60 °C.

Acknowledgments

This work was supported by National Special S&T Project on Water Pollution Control and Management (2017ZX07107002), National Key Research and Development Program (2016YFC0400706), Sino-Canada Cooperation Projects of Tianjin Binhai, Natural Science Foundation of China (no. 21273120 and 51178225) and PICS Project from the French National Center for Scientific Research (CNRS). Lastly, the authors would also like to thank Sophie Chambers for proofreading the manuscript.

Appendix A. Supplementary data

Supplementary data related to this article can be found at https://doi.org/10.1016/j.chemosphere.2018.08.127.

References

Anipsitaks, G.P., Dionysiosd, D.D, 2004. Radical generation by the interaction of transition metals with common oxidants. Environ. Sci. Technol. 38, 3705–3712.

Brillas, E., Boye, B., Sirés, I., Garrido, J.A., Rodrıguez, R.M.a., Arias, C., Cabot, P.-L.s., Comninellis, C., 2004. Electrochemical destruction of chlorophenoxy herbicides by anodic oxidation and electro-Fenton using a boron-doped diamond electrode. Electrochim. Acta 49, 4487–4496.

Bu, L.J., Zhu, S.M., Zhou, S.Q., 2018. Degradation of atrazine by electrochemically activated persulfate using BDD anode: role of radicals and influencing factors. Chemosphere 195, 236–244.

Casado, J., Fornaguera, J., Galan, M.I., 2006. Pilot scale mineralization of organic acids by Electro-Fenton process plus sunlight exposure. Water Res. 40, 2511–2516.

Chen, H., Zhang, Z.L., Feng, M.B., Liu, W., Wang, W.J., Yang, Q., Hu, Y.A., 2017a. Degradation of 2,4-dichlorophenoxyacetic acid in water by persulfate activated with FeS (mackinawite). Chem. Eng. J. 313, 498–507.

Chen, H., Zhang, Z.L., Yang, Z.L., Yang, Q., Li, B., Bai, Z.Y., 2015. Heterogeneous fenton-like catalytic degradation of 2,4-dichlorophenoxyacetic acid in water with FeS. Chem. Eng. J. 273, 481–489.

Chen, X.Q., Murugananthan, M., Zhang, Y.R., 2016. Degradation of p-Nitrophenol by thermally activated persulfate in soil system. Chem. Eng. J. 283, 1357–1365.

Chen, Y., Yan, J.C., Ouyang, D., Qian, L.B., Han, L., Chen, M.F., 2017b. Heterogeneously catalyzed persulfate by CuMgFe layered double oxide for the degradation of phenol. Appl. Catal. Gen. 538, 19–26.

Deng, J., Shao, Y.S., Gao, N.Y., Deng, Y., Zhou, S.Q., Hu, X.H., 2013. Thermally activated persulfate (TAP) oxidation of antiepileptic drug carbamazepine in water. Chem. Eng. J. 228, 765–771.

Devi, P., Das, U., Dalai, A.K., 2016. In-situ chemical oxidation: principle and applications of peroxide and persulfate treatments in wastewater systems. Sci. Total Environ. 571, 643–657.

Ding, D.H., Liu, C., Ji, Y.F., Yang, Q., Chen, L.L., Jiang, C.L., Cai, T.M., 2017. Mechanism insight of degradation of norfloxacin by magnetite nanoparticles activated persulfate: identification of radicals and degradation pathway. Chem. Eng. J. 308, 330–339.

Duan, X.G., Su, C., Zhou, L., Sun, H.Q., Suvorova, A., Odedairo, T., Zhu, Z.H., Shao, Z.P., Wang, S.B., 2016. Surface controlled generation of reactive radicals from persulfate by carbocatalysis on nanodiamonds. Appl. Catal. B Environ. 194, 7–15.

Fang, G.D., Wu, W.H., Liu, C., Dionysiou, D.D., Deng, Y.M., Zhou, D.M., 2017. Activation of persulfate with vanadium species for PCBs degradation: a mechanistic study. Appl. Catal. B Environ. 202, 1–11.

Fang, G.D., Dionysiou, D.D., Wang, Y., Al-Abed, S.R., Zhou, D.M., 2012. Sulfate radical-based degradation of polychlorinated biphenyls: effects of chloride ion and reaction kinetics. J. Hazard Mater. 227–228, 394–401.

Gao, H.P., Chen, J.B., Zhang, Y.B., Zhou, X.F., 2016. Sulfate radicals induced degradation of Triclosan in thermally activated persulfate system. Chem. Eng. J. 306, 522–530.

García, O., Isarain-Chávez, E., Garcia-Segura, S., Brillas, E., Peralta-Hernández, J.M., 2013. Degradation of 2,4-Dichlorophenoxyacetic acid by electro-oxidation and electro-Fenton/BDD processes using a pre-pilot plant. Electrocatalysis 4, 224–234.

George, C., Elrassy, H., Chovelon, J.M., 2001. Reactivity of Selected Volatile Organic Compounds (VOCs) toward the Sulfate Radical ($SO_4^{\bullet-}$), vol. 33. John Wiley & Sons, Inc., pp. 539–547

Anipsitakis, G.P, Dionysiou, D.D., Gonzalez, M.A., 2006. Cobalt-mediated activation of peroxymonosulfate and sulfate radical attack on phenolic compounds. implications of Chloride ions. Environ. Sci. Technol. 40, 1000–1007.

Ghauch, A., Tuqan, A.M., Kibbi, N., 2015. Naproxen abatement by thermally activated persulfate in aqueous systems. Chem. Eng. J. 279, 861–873.

Giri, R.R., Ozaki, H., Ota, S., Taniguchi, S., Takanami, R., 2010. Influence of inorganic solids on photocatalytic oxidation of 2,4-dichlorophenoxyacetic acid with UV and TiO_2 fiber in aqueous solution. Desalination 255, 9–14.

Gu, N., Wu, Y.X., Gao, J.L., Meng, X.Y., Zhao, P., Qin, H.H., Wang, K.T., 2017. Microcystis aeruginosa removal by in situ chemical oxidation using persulfate activated by Fe^{2+} ions. Ecol. Eng. 99, 290–297.

Gu, X.G., Lu, S.G., Li, L., Qiu, Z.F., Sui, Q., Lin, K.F., Luo, Q.S., 2011. Oxidation of 1,1,1-Trichloroethane stimulated by thermally activated persulfate. Ind. Eng. Chem. Res. 50, 11029–11036.

Huy, B.T., Jung, D.S., Kim Phuong, N.T., Lee, Y.I., 2017. Enhanced photodegradation of 2,4-dichlorophenoxyacetic acid using a novel TiO_2@$MgFe_2O_4$ core@shell structure. Chemosphere 184, 849–856.

Jaafarzadeh, N., Ghanbari, F., Ahmadi, M., 2017a. Catalytic degradation of 2,4-dichlorophenoxyacetic acid (2,4-D) by nano-Fe_2O_3 activated peroxymonosulfate: influential factors and mechanism determination. Chemosphere 169, 568–576.

Jaafarzadeh, N., Ghanbari, F., Ahmadi, M., 2017b. Efficient degradation of 2,4-dichlorophenoxyacetic acid by peroxymonosulfate/magnetic copper ferrite nanoparticles/ozone: a novel combination of advanced oxidation processes. Chem. Eng. J. 320, 436–447.

Jia, M.F., Zhang, Z., Li, J.H., Shao, H.J., Chen, L.X., Yang, X.B., 2017. A molecular imprinting fluorescence sensor based on quantum dots and a mesoporous structure for selective and sensitive detection of 2,4-dichlorophenoxyacetic acid. Sensor. Actuator. B Chem. 252, 934–943.

Kang, J., Duan, X.G., Zhou, L., Sun, H.Q., Tadé, M.O., Wang, S.B., 2016. Carbocatalytic activation of persulfate for removal of antibiotics in water solutions. Chem. Eng. J. 288, 399–405.

Kermani, M., Mohammadi, F., Kakavandi, B., Esrafili, A., Rostamifasih, Z., 2018. Simultaneous catalytic degradation of 2,4-D and MCPA herbicides using sulfate radical-based heterogeneous oxidation over persulfate activated by natural hematite (α-Fe_2O_3/PS). J. Phys. Chem. Solid. 117, 49–59.

Kuśmierek, K., Dąbek, L., Świątkowski, A., 2015. A comparative study on oxidative degradation of 2,4-dichlorophenol and 2,4-dichlorophenoxyacetic acid by ammonium persulfate. Desalin. Water Treat. 57, 1098–1106.

Kwan, C.Y., Chu, W., 2004. A study of the reaction mechanisms of the degradation of 2,4-dichlorophenoxyacetic acid by oxalate-mediated photooxidation. Water Res. 38, 4213–4221.

Lam, S.M., Sin, J.C., Abdullah, A.Z., Mohamed, A.R., 2015. Sunlight responsive $WO_{(3)}$/ZnO nanorods for photocatalytic degradation and mineralization of chlorinated phenoxyacetic acid herbicides in water. J. Colloid Interface Sci. 450, 34–44.

Li, K., Wu, J.Q., Jiang, L.L., Shen, L.Z., Li, J.Y., He, Z.H., Wei, P., Lv, Z., He, M.F., 2017a. Developmental toxicity of 2,4-dichlorophenoxyacetic acid in zebrafish embryos. Chemosphere 171, 40–48.

Li, X., Zhou, M.H., Pan, Y.W., Xu, L.T., 2017b. Pre-magnetized Fe^0/persulfate for notably enhanced degradation and dechlorination of 2,4-dichlorophenol. Chem. Eng. J. 307, 1092–1104.

Liang, C.J., Guo, Y.-Y., 2012. Remediation of diesel-contaminated soils using persulfate under alkaline condition. Water, Air, Soil Pollut. 223, 4605–4614.

Liang, C.J., Guo, Y.Y., Pan, Y.R., 2013. A study of the applicability of various activated persulfate processes for the treatment of 2,4-dichlorophenoxyacetic acid. Int. J. Environ. Sci. Technol. 11, 483–492.

Liu, Z.Z., Yang, S.J., Yuan, Y.N., Xu, J., Zhu, Y.F., Li, J.J., Wu, F., 2017. A novel heterogeneous system for sulfate radical generation through sulfite activation on a $CoFe_2O_4$ nanocatalyst surface. J. Hazard Mater. 324, 583–592.

Ma, J., Li, H.Y., Chi, L.P., Chen, H.K., Chen, C.Z., 2017. Changes in activation energy and kinetics of heat-activated persulfate oxidation of phenol in response to changes in pH and temperature. Chemosphere 189, 86–93.

Matzek, L.W., Carter, K.E., 2016. Activated persulfate for organic chemical degradation: a review. Chemosphere 151, 178–188.

Mkhalid, I.A., 2016. Photocatalytic degradation of herbicides under visible light using Pd-WO_3 nanorods. Ceram. Int. 42, 15975–15980.

Nie, M.H., Yan, C.X., Li, M., Wang, X.N., Bi, W.L., Dong, W.B., 2015a. Degradation of chloramphenicol by persulfate activated by Fe^{2+} and zerovalent iron. Chem. Eng. J. 279, 507–515.

Nie, M.H., Yang, Y., Zhang, Z.J., Yan, C.X., Wang, X.N., Li, H.J., Dong, W.B., 2014. Degradation of chloramphenicol by thermally activated persulfate in aqueous solution. Chem. Eng. J. 246, 373–382.

Nie, Y.L., Li, N.N., Hu, C., 2015b. Enhanced inhibition of bromate formation in catalytic ozonation of organic pollutants over Fe–Al LDH/Al_2O_3. Separ. Purif. Technol. 151, 256–261.

Oh, S.Y., Kim, H.W., Park, J.M., Park, H.S., Yoon, C., 2009. Oxidation of polyvinyl alcohol by persulfate activated with heat, Fe^{2+}, and zero-valent iron. J. Hazard Mater. 168, 346–351.

Olmez-Hanci, T., Arslan-Alaton, I., Genc, B., 2013. Bisphenol A treatment by the hot persulfate process: oxidation products and acute toxicity. J. Hazard Mater. 263 Pt 2, 283–290.

Oyama, T., Yanagisawa, I., Takeuchi, M., Koike, T., Serpone, N., Hidaka, H., 2009. Remediation of simulated aquatic sites contaminated with recalcitrant substrates by TiO_2/ozonation under natural sunlight. Appl. Catal. B Environ. 91, 242–246.

Pan, Y.W., Zhou, M.H., Li, X., Xu, L.T., Tang, Z.X., Liu, M.M., 2016. Novel Fenton-like process (pre-magnetized Fe^0/H_2O_2) for efficient degradation of organic pollutants. Separ. Purif. Technol. 169, 83–92.

Peng, H.J., Zhang, W., Xu, L.Y., Fu, R.B., Lin, K.F., 2016a. Oxidation and mechanism of decabromodiphenyl ether (BDE209) by thermally activated persulfate (TAP) in a soil system. Chem. Eng. J. 306, 226–232.

Peng, L.B., Wang, L., Hu, X.T., Wu, P.H., Wang, X.Q., Huang, C.M., Deng, D.Y., 2016b. Ultrasound assisted, thermally activated persulfate oxidation of coal tar DNAPLs. J. Hazard Mater. 318, 497–506.

Qiu, P.X., Yao, J.H., Chen, H., Jiang, F., Xie, X.C., 2016. Enhanced visible-light photocatalytic decomposition of 2,4-dichlorophenoxyacetic acid over $ZnIn_2S_4$/g-C_3N_4 photocatalyst. J. Hazard Mater. 317, 158–168.

Rao, Y.F., Chu, W., Wang, Y.R., 2013. Photocatalytic oxidation of carbamazepine in triclinic-WO_3 suspension: role of alcohol and sulfate radicals in the degradation pathway. Appl. Catal. A Gen. 468, 240–249.

Rodríguez, J.L., Valenzuela, M.A., Tiznado, H., Poznyak, T., Chairez, I., Magallanes, D., 2017. A comparative study of alumina-supported Ni catalysts prepared by photodeposition and impregnation methods on the catalytic ozonation of 2,4-dichlorophenoxyacetic acid. J. Nanoparticle Res. 19, 54.

Singh, R.K., Philip, L., Ramanujam, S., 2017. Removal of 2,4-dichlorophenoxyacetic acid in aqueous solution by pulsed corona discharge treatment: effect of different water constituents, degradation pathway and toxicity assay. Chemosphere 184, 207–214.

Souza, F.L., Saéz, C., Lanza, M.R.V., Cañizares, P., Rodrigo, M.A., 2016. Removal of pesticide 2,4-D by conductive-diamond photoelectrochemical oxidation. Appl. Catal. B Environ. 180, 733–739.

Wang, S.L., Zhou, N., Wu, S., Zhang, Q., Yang, Z., 2015. Modeling the oxidation kinetics of sono-activated persulfate's process on the degradation of humic acid. Ultrason. Sonochem. 23, 128–134.

Wang, Q.F., Shao, Y.S., Gao, N.Y., Chu, W.H., Shen, X., Lu, X., Chen, J.X., Zhu, Y.P., 2016.

Degradation kinetics and mechanism of 2,4-Di-tert-butylphenol with UV/persulfate. Chem. Eng. J. 304, 201–208.
Xiao, H.S., Lv, B.Y., Gao, J.X., Zhao, G.H., 2016. Hydrothermal electrocatalytic oxidation for the treatment of herbicides wastewater. Environ. Sci. Pollut. Res. Int. 23, 10050–10057.
Xu, L.J., Wang, J.L., 2012. Fenton-like degradation of 2,4-dichlorophenol using Fe_3O_4 magnetic nanoparticles. Appl. Catal. B Environ. 123–124, 117–126.
Yang, J.F., Yang, L.M., Zhang, S.B., Ou, L.H., Liu, C.B., Zheng, L.Y., Yang, Y.F., Ying, G.G., Luo, S.L., 2017. Degradation of azole fungicide fluconazole in aqueous solution by thermally activated persulfate. Chem. Eng. J. 321, 113–122.
Ye, J.S., Liu, J., Ou, H.S., Wang, L.L., 2016. Degradation of ciprofloxacin by 280 nm ultraviolet-activated persulfate: degradation pathway and intermediate impact on proteome of Escherichia coli. Chemosphere 165, 311–319.
You, B., Jiang, N., Sheng, M.L., Drisdell, W.S., Yano, J., Sun, Y.J., 2015. Bimetal-organic framework self-adjusted synthesis of support-free nonprecious electrocatalysts for efficient oxygen reduction. ACS Catal. 5, 7068–7076.
Zhao, G.H., Li, P.Q., Nong, F.Q., Li, M.F., Gao, J.X., Li, D.M., 2010. Construction and high performance of a novel modified boron-doped diamond film electrode endowed with superior electrocatalysis. J. Phys. Chem. C 114, 5906–5913.
Zhao, L., Ji, Y.F., Kong, D.Y., Lu, J.H., Zhou, Q.S., Yin, X.M., 2016. Simultaneous removal of bisphenol A and phosphate in zero-valent iron activated persulfate oxidation process. Chem. Eng. J. 303, 458–466.
Zhu, K.R., Baig, S.A., Xu, J., Sheng, T.T., Xu, X.H., 2012. Electrochemical reductive dechlorination of 2,4-dichlorophenoxyacetic acid using a palladium/nickel foam electrode. Electrochim. Acta 69, 389–396.